



Miocene calc-alkaline volcanism in southern Jackson Hole, Wyoming : evidence of subduction-related volcanism

by David Congdon Adams

A thesis submitted in partial fulfillment of the requirements for the degree of Master of Science in Earth Sciences

Montana State University

© Copyright by David Congdon Adams (1997)

Abstract:

Late Miocene lava flows in southern Jackson Hole are distinctly intermediate, calc-alkaline in composition in contrast to the bimodal basalt-rhyolite assemblages characteristic of most Neogene volcanic rocks in the Yellowstone Plateau-Snake River Plain region. Despite limited stratigraphic continuity between units, geochemical and petrographic analysis reveals strongly unifying and distinctive features. Silica variation diagrams are remarkably coherent, suggesting a co-genetic, if not co-magmatic, origin. As a whole, these rocks are significantly lower in K and Fe and higher in Ca and especially Mg than rocks of similar silica content from the Snake River Plain and Yellowstone. The basaltic andesites in particular are characterized by abundant olivine phenocrysts (Po 80-90) and extremely high Ni (200 ppm) and Cr (550 ppm) values. Within the suite, basaltic andesites and andesites (54-58% SiO₂, with olivine and augite) differ from dacites (60-62% SiO₂, aphyric or hornblende-rich) which differ from rhyodacites (66-69% SiO₂, with hypersthene and rounded andesine) and rhyolites and obsidian (73-75% SiO₂). Both geochemical and petrographic features suggest involvement of varying degrees of crustal contamination and/or magma mixing, especially in the more silicic rocks.

Low ¹⁴³Nd/¹⁴⁴Nd ratios in this suite clearly distinguish it from the Yellowstone-Snake River Plain volcanics and suggest the absence of asthenospheric input, precluding melt generation due to convective heat transfer. A possible melting mechanism is suggested by the high Ba/Nb values of these rocks, a feature considered diagnostic of involvement of subducted slab-derived hydrous flux in melt generation. It is proposed that a fragment of subducted slab detached as the Cascade subduction zone was disrupted by the inception of the Yellowstone mantle plume was buoyed and transported eastward, where its descent and dehydration beneath western Wyoming produced calc-alkaline magmas by solidus depression in the lithospheric mantle and lower crust.

MIOCENE CALC-ALKALINE VOLCANISM IN SOUTHERN JACKSON HOLE,
WYOMING: EVIDENCE OF SUBDUCTION-RELATED VOLCANISM

by

David Congdon Adams

A thesis submitted in partial fulfillment
of the requirements for the degree

of

Master of Science

in

Earth Sciences

MONTANA STATE UNIVERSITY-BOZEMAN
Bozeman, Montana

May 1997

N378
Ad 16

APPROVAL

of a thesis submitted by

David Congdon Adams

This thesis has been read by each member of the thesis committee and has been found to be satisfactory regarding content, English usage, format, citations, bibliographic style, and consistency, and is ready for submission to the College of Graduate Studies.

Dr. David R. Lageson

D.R. Lageson 4-17-97
Date

Approved for the Department of Earth Sciences

Dr. W. Andrew Marcus

W. Andrew Marcus 4-17-97
Date

Approved for the College of Graduate Studies

Dr. Robert L. Brown

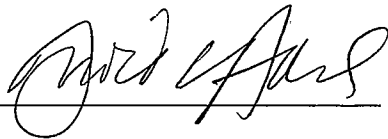
R.L. Brown 4/20/97
Date

STATEMENT OF PERMISSION TO USE

In presenting this thesis in partial fulfillment of the requirements for a master's degree at Montana State University-Bozeman, I agree that the Library shall make it available to borrowers under rules of the Library.

If I have indicated my intention to copyright this thesis by including a copyright notice page, copying is allowable only for scholarly purposes, consistent with "fair use" as prescribed by the U.S. Copyright Law. Requests for permission for extended quotation from or reproduction of this thesis in whole or in parts may be granted only by the copyright holder.

Signature

A handwritten signature in cursive script, appearing to read "David A. ...", written over a horizontal line.

Date

4-15-97

TABLE OF CONTENTS

	Page
1. INTRODUCTION.....	1
Overview.....	1
Subduction Geochemistry.....	4
Regional Setting.....	9
2. STUDY AREA.....	14
Structural Overview.....	14
Previous Work.....	18
Distribution of Volcanic Rocks.....	19
3. MATERIALS AND METHODS.....	23
4. RESULTS.....	24
Overview.....	24
Locations and Field Characteristics.....	25
Basaltic Andesites.....	25
Low-silica Andesites.....	28
Trachyandesites.....	30
High-silica Andesites.....	30
Dacites.....	33
Rhyolites.....	35
Petrography.....	38
Basaltic Andesites.....	38
Low-silica Andesites.....	40
Trachyandesites.....	42
High-silica Andesites.....	43
Dacites.....	43
Rhyolites.....	47
Geochemistry.....	47
Overview.....	47
Major elements variations.....	49

Trace element variations.....	54
Isotopes.....	63
5. DISCUSSION.....	69
Overview.....	69
Magma Mixing.....	70
Fractionation and Assimilation (AFC).....	76
Source Rocks and their History.....	81
Processes Responsible for Initial Melting.....	88
Extensional Decompression Melting.....	88
Crustal Thickening.....	89
Injection of Hot Mantle.....	90
Slab-derived Hydrous Fluxes.....	92
Tectonic Setting.....	95
6. CONCLUSIONS.....	103
REFERENCES CITED.....	105
APPENDIX.....	125

LIST OF TABLES

	Page
Table 1. Major and trace element contents and isotope ratios for basaltic andesite samples.....	27
Table 2. Major and trace element contents and isotope ratios for low-silica andesite samples.....	29
Table 3. Major and trace element contents and isotope ratios for trachyandesite samples.....	31
Table 4. Major and trace element contents and isotope ratios for high-silica andesite samples.....	32
Table 5. Major and trace element contents and isotope ratios for dacite samples.	34
Table 6. Major and trace element contents and isotope ratios for rhyolite samples.	36

LIST OF FIGURES

	Page
Figure 1. Structural index map of the Teton Range.....	15
Figure 2. Map of study area.....	17
Figure 3. Total alkali vs. SiO ₂ classification plot.....	25
Figure 4. Photomicrograph of Sample JH1.....	39
Figure 5. Photomicrograph of Sample 81.....	39
Figure 6. Photomicrograph of Sample 625.....	41
Figure 7. Photomicrograph of Sample 606.....	41
Figure 8. Photomicrograph of Sample JH6.....	44
Figure 9. Photomicrograph of Sample JH6.....	44
Figure 10. Photomicrograph of Sample 32.....	45
Figure 11. Photomicrograph of Sample SM2.....	46
Figure 12. Photomicrograph of Sample JH12.....	46
Figure 13. Plot of Al ₂ O ₃ vs. SiO ₂ (wt. %).	48
Figure 14. Plot of TiO ₂ vs. SiO ₂ (wt. %).	48
Figure 15. Plot of FeO* vs. SiO ₂ (wt. %).	50
Figure 16. Plot of MnO vs. SiO ₂ (wt. %).	50
Figure 17. Plot of CaO vs. SiO ₂ (wt. %).	51

Figure 18. Plot of MgO vs. SiO ₂ (wt. %)	52
Figure 19. Plot of K ₂ O vs. SiO ₂ (wt. %)	52
Figure 20. Plot of Na ₂ O vs. SiO ₂ (wt. %)	53
Figure 21. Plot of P ₂ O ₅ vs. SiO ₂ (wt. %)	53
Figure 22. Plot of Ni (ppm.) vs. SiO ₂ (wt. %)	55
Figure 23. Plot of Cr (ppm.) vs. SiO ₂ (wt. %)	55
Figure 24. Plot of Sc (ppm.) vs. SiO ₂ (wt. %)	56
Figure 25. Plot of V (ppm.) vs. SiO ₂ (wt. %)	56
Figure 26. Plot of Ba (ppm.) vs. SiO ₂ (wt. %)	57
Figure 27. Plot of Rb (ppm.) vs. SiO ₂ (wt. %)	57
Figure 28. Plot of Sr (ppm.) vs. SiO ₂ (wt. %)	59
Figure 29. Plot of Zr (ppm.) vs. SiO ₂ (wt. %)	59
Figure 30. Plot of Y (ppm.) vs. SiO ₂ (wt. %)	60
Figure 31. Plot of La (ppm.) vs. SiO ₂ (wt. %)	60
Figure 32. Plot of Ce (ppm.) vs. SiO ₂ (wt. %)	61
Figure 33. Plot of Pb (ppm.) vs. SiO ₂ (wt. %)	61
Figure 34. Plot of Th (ppm.) vs. SiO ₂ (wt. %)	62
Figure 35. Plot of Nb (ppm.) vs. SiO ₂ (wt. %)	62
Figure 36. Plot of ¹⁴³ Nd/ ¹⁴⁴ Nd vs. ⁸⁷ Sr/ ⁸⁶ Sr	64
Figure 37. Plot of ¹⁴³ Nd/ ¹⁴⁴ Nd vs. SiO ₂	64
Figure 38. Plot of ⁸⁷ Sr/ ⁸⁶ Sr vs. SiO ₂	65

Figure 39. Plot of $^{207}\text{Pb}/^{204}\text{Pb}$ vs. $^{206}\text{Pb}/^{204}\text{Pb}$	65
Figure 40. Plot of $^{208}\text{Pb}/^{204}\text{Pb}$ vs. $^{206}\text{Pb}/^{204}\text{Pb}$	66
Figure 41. Plot of $^{206}\text{Pb}/^{204}\text{Pb}$ vs. SiO_2	66
Figure 42. Plot of $^{207}\text{Pb}/^{204}\text{Pb}$ vs. SiO_2	67
Figure 43. Plot of $^{208}\text{Pb}/^{204}\text{Pb}$ vs. SiO_2	67
Figure 44. Plot of MgO vs. SiO_2 (wt. %).	73
Figure 45. Plot of Ni vs. SiO_2 (ppm, wt. %).	73
Figure 46. Plot of Cr vs. SiO_2 (ppm, wt. %).	74
Figure 47. Plot of Sr vs. Rb (ppm).	74
Figure 48. Plot of Rb vs. Th (ppm).	75
Figure 49. Plot of K/Rb vs. SiO_2 (ppm, wt. %).	75
Figure 50. Plot of Pearce element ratios for JHV andesites and basaltic andesites.	80
Figure 51. Plot of Pearce element ratios for the JHV.....	80
Figure 52. Plot of $^{143}\text{Nd}/^{144}\text{Nd}$ vs. $^{87}\text{Sr}/^{86}\text{Sr}$	85
Figure 53. Plot of $^{87}\text{Sr}/^{86}\text{Sr}$ vs. Sr (ppm).....	85
Figure 54. Plot of $^{207}\text{Pb}/^{204}\text{Pb}$ vs. $^{206}\text{Pb}/^{204}\text{Pb}$	86
Figure 55. Plot of $^{208}\text{Pb}/^{204}\text{Pb}$ vs. $^{206}\text{Pb}/^{204}\text{Pb}$	86
Figure 56. Plot of Ba/Nb (ppm) vs. SiO_2	93
Figure 57. Models relating Cascade volcanism, Columbia River Basalt eruption, and the Yellowstone mantle plume.	98
Figure 58. Cartoon depicting the sequence and relationship of magmatic and tectonic events in the northwestern United States during the late Cenozoic.....	99-100

ABSTRACT

Late Miocene lava flows in southern Jackson Hole are distinctly intermediate, calc-alkaline in composition in contrast to the bimodal basalt-rhyolite assemblages characteristic of most Neogene volcanic rocks in the Yellowstone Plateau-Snake River Plain region. Despite limited stratigraphic continuity between units, geochemical and petrographic analysis reveals strongly unifying and distinctive features. Silica variation diagrams are remarkably coherent, suggesting a co-genetic, if not co-magmatic, origin. As a whole, these rocks are significantly lower in K and Fe and higher in Ca and especially Mg than rocks of similar silica content from the Snake River Plain and Yellowstone. The basaltic andesites in particular are characterized by abundant olivine phenocrysts (Fo 80-90) and extremely high Ni (200 ppm) and Cr (550 ppm) values. Within the suite, basaltic andesites and andesites (54-58% SiO₂, with olivine and augite) differ from dacites (60-62% SiO₂, aphyric or hornblende-rich) which differ from rhyodacites (66-69% SiO₂, with hypersthene and rounded andesine) and rhyolites and obsidian (73-75% SiO₂). Both geochemical and petrographic features suggest involvement of varying degrees of crustal contamination and/or magma mixing, especially in the more silicic rocks.

Low ¹⁴³Nd/¹⁴⁴Nd ratios in this suite clearly distinguish it from the Yellowstone-Snake River Plain volcanics and suggest the absence of asthenospheric input, precluding melt generation due to convective heat transfer. A possible melting mechanism is suggested by the high Ba/Nb values of these rocks, a feature considered diagnostic of involvement of subducted slab-derived hydrous flux in melt generation. It is proposed that a fragment of subducted slab detached as the Cascade subduction zone was disrupted by the inception of the Yellowstone mantle plume was buoyed and transported eastward, where its descent and dehydration beneath western Wyoming produced calc-alkaline magmas by solidus depression in the lithospheric mantle and lower crust.

CHAPTER 1

INTRODUCTION

Overview

Cenozoic volcanism in the interior regions of the western United States has been extensive and has exhibited a wide range in geochemical character (Lipman, 1992; Luedke and Smith, 1978a-e). In their seminal papers, Christiansen and Lipman(1972) and Lipman et al. (1972) identified two general tectono-magmatic associations: an early calc-alkaline, predominantly andesitic episode attributed to shallow subduction of the Farallon Plate and a later period of basaltic, bimodal, or “fundamentally basaltic” volcanism associated with regional extension. They also noticed broad spatial trends in the timing of the transition from one association to the other, attributed to the gradual replacement of the coastal subduction zone with a transform boundary. However, owing to the fairly ambiguous nature of the geochemical nature of the later group, this transition is not always clear, especially in the northern portions of the region, where subduction presently continues off the Oregon and Washington coasts. Many volcanic fields elsewhere in the western United States also do not fit neatly into either category (e.g. the Jemez in New Mexico (Perry et al., 1987)).

Christiansen and Lipman (1972) purposely refrained from proposing a petrogenetic explanation for these tectonic-geochemical relationships and never implied any paleostress

aspects to the earlier subduction-related trend. Subsequent workers, however, have assumed a "compressional" tectonic character for subduction environments and claim to identify the timing of a shift from "compressional" to extensional tectonism in particular locales (Barnosky, 1984; McDowell and Fritz, 1995). It is not clear that Lipman and Christiansen intended a paleostress interpretation for this geochemical transition, and they also acknowledged the difficulty in applying these concepts to individual areas as opposed to regions.

Stress in volcanic arcs can range from tensional in the backarc to compressional in the arc and forearc. Present-day stress fields in the Pacific Northwest also show a dominant component of dextral shear oblique to the arc axis (Zoback and Zoback, 1989). Indeed, the arc and forearc regions of any subduction environment may experience extension if the rate of slab rollback exceeds that of plate convergence (Royden, 1993).

The association of compressional paleostress with intermediate volcanism stems from early theories in which basaltic melts would be trapped in crustal magma chambers, as contraction closed available conduits. In such chambers, differentiation and crustal assimilation produces andesitic magmas. Extensional paleostrain would allow basaltic melts to pass unaffected through the crust (Hildreth, 1981; Norman and Leeman, 1989). Subsequent experimental work on andesites (Green 1973, 1982; Egger, 1972, 1974; Egger and Burnham, 1973) has suggested that certain conditions of partial melting (such as high water content) are perhaps more important than fractionation in the genesis of andesitic volcanism, especially as regards arc magmatism. In certain circumstances such

as the Mogollon-Datil volcanic field (Cather, 1990), such a relationship between stress and volcanism may be realistic. However, in no way should the mere presence of extensional tectonism be taken as evidence precluding the possibility of subduction-related volcanism as some authors seem to suggest (Hooper et al., 1995).

Continued work on Cenozoic andesitic volcanism in the western United States has shown that, in many areas, lavas of intermediate composition can be generated by magma mixing (McMillan and Dungan, 1988; Gerlach and Grove, 1982) or crustal assimilation (Gans et al., 1989) without necessarily requiring subduction of oceanic crust and that shifts in gross geochemistry may be a normal part of open-system magmatic evolution. Significant amounts of basalt can also occur in areas such as the Cascades, where subduction is indisputably the dominant tectonic process (Leeman et al., 1990; McBirney et al., 1974). Studies of bimodal volcanism have emphasized the primary importance of upwelling of asthenospheric mantle in areas of both significant (Suneson and Lucchitta, 1983) and minimal extension (Leeman, 1982a).

It thus appears that intermediate composition volcanism need not indicate subduction and that basaltic or bimodal volcanism need not preclude it. Instead, detailed study of each particular case is required, especially given the tectonic complexity of the western United States and the heterogeneity of its lithosphere, both crust and mantle (Menzies et al., 1983; Menzies, 1989; Lum et al., 1989). As pointed out by Arculus and Johnson (1978), there has often been an overemphasis on generalized models thereby ignoring the valuable information to be gained from the unique aspects of individual case

histories. In this regard, it is also preferable that traditionally accepted geochemical subduction signatures (Gill, 1981) be critically examined to ascertain their applicability in this more or less intracontinental setting (Arculus, 1987).

Subduction Geochemistry

Crucial to Christiansen and Lipman's (1972) division of Cenozoic volcanism in the western United States, and the spatio-temporal trends displayed thereby, is not the distinction between extensional and compressional tectonism nor intermediate and basaltic or bimodal lavas. *Instead, it is the presence or absence of subduction-related volcanism.*

Following Christiansen and Lipman's 1972 paper, considerable work has been done on the geochemical aspects of subduction as expressed in arc magmas. Major and trace element contents in subduction-related volcanic rocks have been summarized by Jakes and White (1973), Ewart (1982), and Pearce (1982). Isotope systematics have been summarized by Hawkesworth (1982). Based on these features, various discriminant diagrams have been developed to distinguish arc magmas from those of other tectonic settings.

Primary among these features is the general depletion in subduction-related lavas of high field strength elements (HFSE, e.g., Ti, Hf, Nb, Ta) relative to large ion lithophile elements (LILE, e.g., Rb, Cs, Ba, K). These two groups show similarly incompatible

behavior in crystal fractionation processes; however, LILE partition much more readily into a hydrous phase (Pearce and Norry, 1979; Tatsumi et al., 1986). Some workers (Eggler, 1987) have found little or no LILE vs. HFSE fractionation in hydrous systems. However, Eggler's findings involve the derivation of fluid-crystal partitioning data from the combination of fluid-melt and melt-crystal partitioning data; whereas Tatsumi directly observed fluid-crystal partitioning in the dehydration of spiked synthetic serpentine. Gill (1981) asserted that "a Ba/Ta ratio greater than 450 ($Ba/Nb > \sim 25$) is the single most diagnostic characteristic of arc magma." Although HFSE depletion has also been attributed to the stabilization, in either the slab or mantle wedge, of a residual phase such as rutile (Ryerson and Watson, 1987) or fractionation of other minor mineral phases (Saunders et al., 1980), the most widely accepted explanation is the enrichment and melting of the overlying mantle wedge by a flux derived from a descending and dehydrating oceanic crustal slab (Hooper and Hawkesworth, 1993). The question remains of the relative content of hydrous fluid versus silicate melt in this slab-derived flux (Arculus, 1987). Ratios such as K/Ti (Kempton et al., 1991) and Nb/Ta (Stolz et al., 1996) have been used to determine the relative importance of these two metasomatic modes.

Although such features have been used to assign an arc setting to rocks as old as the Precambrian (Pearce and Cann, 1973), in Tertiary volcanics of the western United States, they are often briefly acknowledged and then dismissed usually due to excessive distance from and/or non-alignment with potential coastal subduction zones (Robyn, 1979;

Goles, 1986; Gans et al., 1989). In the case of many recent studies, consideration of the process of initial melt generation is essentially ignored in favor of concentrating on subsequent aspects of magma evolution.

What then would constitute sufficient evidence of subduction-related volcanism in the interior of the western United States? Ratios such as Ba/Nb, although compelling, can be of dubious significance in the more alkalic provinces, where, for reasons other than slab dehydration, LILE values can be extreme (Dudas, pers. comm.). More importantly, much of the lithospheric mantle underlying the western U.S. may have experienced one or more episodes of subduction-related metasomatism; thus the geochemical characteristics of subduction may be *inherited* rather than the result of contemporaneous slab dehydration.

It is clear that in addition to evidence of slab dewatering metasomatism, evidence of *melt generation* by hydrous flux depression of solidus temperatures must also be established. The other options for melting the lithosphere are adiabatic decompression due to rapid extension, heat input from the asthenosphere, or increase in burial depth due to tectonic crustal thickening. Decompression melting requires substantial rates of crustal extension (McKenzie and Bickle, 1988; White and McKenzie, 1989) that are seldom encountered outside of mid-ocean ridges or continental rift zones, where "passive" upwelling of asthenosphere can occur. Upwelling of asthenospheric mantle also occurs without major extensional tectonism in association with mantle plumes, or "hot spots", which melt the lithosphere by conductive and/or convective thermal input.

The question of the relative amount of incorporation of asthenospheric mantle material in melts generated in the Cenozoic in the western United States is a very important one, as it can provide constraints on the possible mechanisms of initial melting. In other words, in regions where the geochemical signature of the asthenospheric (i.e. convecting) mantle can be distinguished, the absence of said signature would tend to preclude melting mechanisms that require heat input by advection of hot asthenospheric material. Lachenbruch and Sass (1978) pointed out that "the ultimate source of high heat flow in the Basin and Range province must be upward convective transport in the asthenosphere." Under these conditions, McKenzie and Bickle (1988) have shown that the first point of intersection of the geotherm with solidus (i.e. melting) will always occur at the transition from the conductive to the adiabatic geotherm at the base of the thermal boundary (i.e. within the asthenosphere).

Some workers (Christiansen and McKee, 1978; Dudas, 1991; Hooper et al., 1995) have suggested that melting entirely within the lithosphere could be induced by extension, perhaps with some degree of conductive pre-heating from the asthenosphere. However, decompression is the vital component of this process; thus the lithosphere would need to undergo either extensive removal of crustal overburden (increasing heat loss due to steepening of the conductive geotherm) or diapiric upwelling. The latter would require, at the outset, a density contrast, presumably thermally induced, between the diapir and its surrounding material. As much of the material above the developing diapir would be of increasingly lower- density crustal nature, it is not clear how extension could trigger this

process. In any event, as outlined earlier, an asthenospheric melt would already be present due to extension-induced upwelling (McKenzie and Bickle, 1988); thus any lithospheric melting would more likely be the result of direct contact with intruding or underplating asthenospheric melts, most probably leading to some asthenospheric signature in the resulting magmas. This positive relationship between amount of extension and asthenospheric input has been noted in Rio Grande Rift lavas (Perry et al., 1987).

Leeman (1982b) has proposed a purely lithospheric source for the Snake River Plain tholeiitic basalts and the associated rhyolites in a setting involving minimal extension but dominated by high heat flow from an upwelling mantle plume (Leeman, 1982a). Once again, deriving sufficient heat from hot, convecting asthenospheric mantle to melt the lithosphere in such large volumes without asthenospheric admixture seems improbable. In fact, Menzies (1989) includes a small amount of OIB (ocean island basalt) type mantle as a component of these magmas, acknowledging the inevitability of some asthenospheric admixture during heat transfer. Based on low seismic velocities to depths of 250 km. and a high ^3He flux at Yellowstone, Hildreth et al. (1991) also suggested sublithospheric magma contributions.

The prevailing model for melt generation in volcanic arcs does not involve the asthenosphere as a source of heat; rather it is solidus depression due to slab-derived hydrous fluxes that initiates melting. Nonetheless, in the majority of arc settings, the nature of the mantle wedge in which the melting occurs is convecting, asthenospheric mantle. Only in situations in which the descending slab is directly overlain by lithospheric

mantle would the resulting melt contain no evidence of asthenospheric input. Some workers have suggested that a convecting mantle wedge is necessary in order to transport mantle metasomatized by shallow slab-derived fluxes to deeper, hotter levels appropriate for melting (Tatsumi, 1989). Indeed, areas in the Andean arc where shallow subduction is apparently taking place and where the slab is interpreted to be in direct contact with the lithosphere (Sacks, 1983) are distinctly non-volcanic. Nevertheless, this lack of volcanism could just as well be due to the lack of correct pressure and temperature conditions for slab dehydration or lithospheric melting as due to the absence of asthenospheric mantle per se.

In summary, in areas such as Yellowstone and the surrounding region where an asthenospheric signature can be determined with a reasonable amount of certainty, lavas lacking that signature strongly suggest the possibility of the involvement of slab-derived fluids in the melting of the lithosphere.

Regional Setting

Northwest Wyoming and the surrounding region has experienced a complex magmatic and tectonic history during the Cenozoic. Sevier and Laramide-style contractional tectonism spanned a period from the late Cretaceous to the Eocene, during which extensive calc-alkaline and alkalic volcanism produced the Challis, Absaroka, and Central Montana volcanic provinces. These provinces, and the Sevier and Laramide

orogenies themselves, have been attributed to the shallow subduction of the Farallon Plate beneath the western portion of the North American Plate (e.g. Lipman et al., 1972; Snyder et al., 1976). Other workers (Fitton et al., 1991; Hooper et al., 1995) have suggested that the geochemical subduction signature of these lavas is inherited from the metasomatized mantle of the accreted arc terranes which make up most of the western U.S., including portions of the Archaean Wyoming craton (Dudas, 1991).

Since the early Miocene the region has been dominated by a northeast-propagating system of explosive, rhyolitic volcanism followed by extrusion of basalt without any intermediate lavas (Pierce and Morgan, 1992). The present locus of explosive activity is in Yellowstone National Park and vicinity, where caldera-forming eruptions have occurred at 2.0, 1.3, and 0.6 Ma (Hildreth et al., 1991; Christiansen, 1995). To the west, the distribution of various widespread ash-fall tuffs suggest the presence of earlier calderas; in the vicinity of Rexburg, Idaho, 6.6 to 4.3 Ma (Morgan et al., 1984; Morgan and Hackett, 1988; Morgan, 1992); and in the general vicinity of Twin Falls, Idaho, ~10 to ~8 Ma (Leeman, 1982c). The system can be traced back as far as the McDermitt volcanic field (~16 Ma.) in the Owhyee Mountains in eastern Oregon (Pierce and Morgan, 1992).

Although the region has, during the Neogene, been experiencing a very general, eastward-propagating front of "Basin and Range" extension (Rodgers et al., 1990), it appears that the developing magmatic system has also confined the distribution of extensional tectonism to a parabolic or "bow wave" pattern (Anders et al., 1989; Anders and Sleep, 1992). In addition, a sequence of initial regional uplift followed by subsidence

can be seen associated with the eastward migration of explosive rhyolitic activity (Fritz and Sears, 1993; Smith and Braile, 1994).

The interpretations of the Snake River Plain-Yellowstone province and this eastward-propagating magmatic system are numerous, but only one substantially explains the tectonic, geochemical, and isotopic evidence. Interpreting the Plain as an eastward-propagating extensional rift (Myers and Hamilton, 1964) is contrary to overwhelming evidence of an extensional direction parallel to the axis of the Plain (Allmendinger, 1982; Kuntz et al., 1992). Reactivation of an ancient plain of weakness (Eaton et al., 1975; Mabey et al., 1978) or characterization as a "leaky transform" between regions of differing rates of extension (Christiansen and McKee, 1978) may explain the overall geometry of the province but fail even to begin to consider the localization or the nature of the region's magmatism.

Only a model involving a deep-seated upwelling of asthenospheric mantle or "mantle plume" fully treats the time-transgressive nature of the magmatism (Armstrong et al., 1975), its large volume and geochemical features (Leeman, 1982c), regional heat flow (Brott et al., 1981; Blackwell, 1989), the deep-mantle signature of the He^3/He^4 ratios (Craig et al., 1978; Kennedy et al., 1987), and regional uplift and subsidence (Fritz and Sears, 1993; Pierce and Morgan, 1992). For this reason, the subcrustal mechanism responsible for the Snake River Plain-Yellowstone volcanic province will herein be referred to as a mantle plume rather than some other, more coy and obfuscatory term.

Under the mantle plume model, a broad plume "head" produced a regional epeirogenic uplift and possibly affected volcanic activity as far east as Colorado (Leat et al., 1991). This plume head may have produced (Draper, 1991; Geist and Richards, 1993), strongly influenced (Hooper, 1990; Hooper and Hawkesworth, 1993), or had no effect on the Columbia River Basalts (Carlson and Hart, 1987; Hart and Carlson, 1987). The more narrowly focused plume "tail" subsequently produced the eastern Snake River Plain and Yellowstone Plateau as the North American plate drifted to the west-southwest over the essentially stationary plume (Pierce and Morgan, 1992). Basaltic melts derived from the ascending, superheated mantle caused extensive anatexis in the lower crust. These rhyolitic melts not only led to explosive, caldera-forming eruptions by the formation and catastrophic draining of upper crustal magma chambers, but they also served as a low-density cap blocking the ascent of the denser basalts (Leeman, 1982c; Anders and Sleep, 1992). Only around the periphery of the province or after the rhyolite had cooled sufficiently to allow brittle fracture, could the less viscous basalt exploit the resulting conduits and reach the surface (Hildreth et al., 1991; Kuntz, 1992). This bimodal magmatism, rhyolite followed by basalt with no intermediate compositions, dominates the province; although some "hybrid" ferrobasalts and ferrolatites (Leeman, 1982d) and evidence of basalt-rhyolite mixing (Wilcox, 1944) do exist.

In the area of southern Jackson Hole, Wyoming, approximately 70 km south of Yellowstone National Park, there exist, however, scattered outcrops of late-Miocene intermediate lava flows. Not only are these volcanics distinctly not bimodal, but, as will be

shown in subsequent chapters, their major and trace elements and isotopic ratios also indicate that they can in no way be derived from the magmas of the Yellowstone-Snake River Plain system. In addition, nowhere in the literature, to the author's knowledge, is there mention of a similar Neogene volcanic suite in the region. These lavas, herein referred to as the Jackson Hole volcanic complex (JHV), are apparently unique.

CHAPTER 2

STUDY AREA

Structural Overview

Jackson Hole, in northwestern Wyoming, is a north-trending, flat-bottomed valley approximately 12 km wide by 75 km long. (Figure 1) It is flanked on the east, from north to south, by the Pinyon Highlands, Leidy Peak Highlands, Gros Ventre Range, and Hoback Range. On the west it is flanked from north to south by the Teton Range and Snake River Range.

For most of its length, the valley is a half graben which constitutes the downdropped hanging-wall block of the east-dipping Teton normal fault. At its southern end, the half graben is reversed, with the master fault, the west-dipping Hoback normal fault, lying on the eastern side of the valley. The transition between the two half grabens coincides with two opposing WNW-trending thrust faults which mark the boundary between two major structural provinces. To the north, the Teton and Gros Ventre Ranges and the intervening valley occupy the hanging wall of the Cache Creek thrust, a thick-skinned, basement-cored, Laramide-style contractional fault. To the south, the Snake River and Hoback Ranges and intervening valley occupy the hanging walls of several

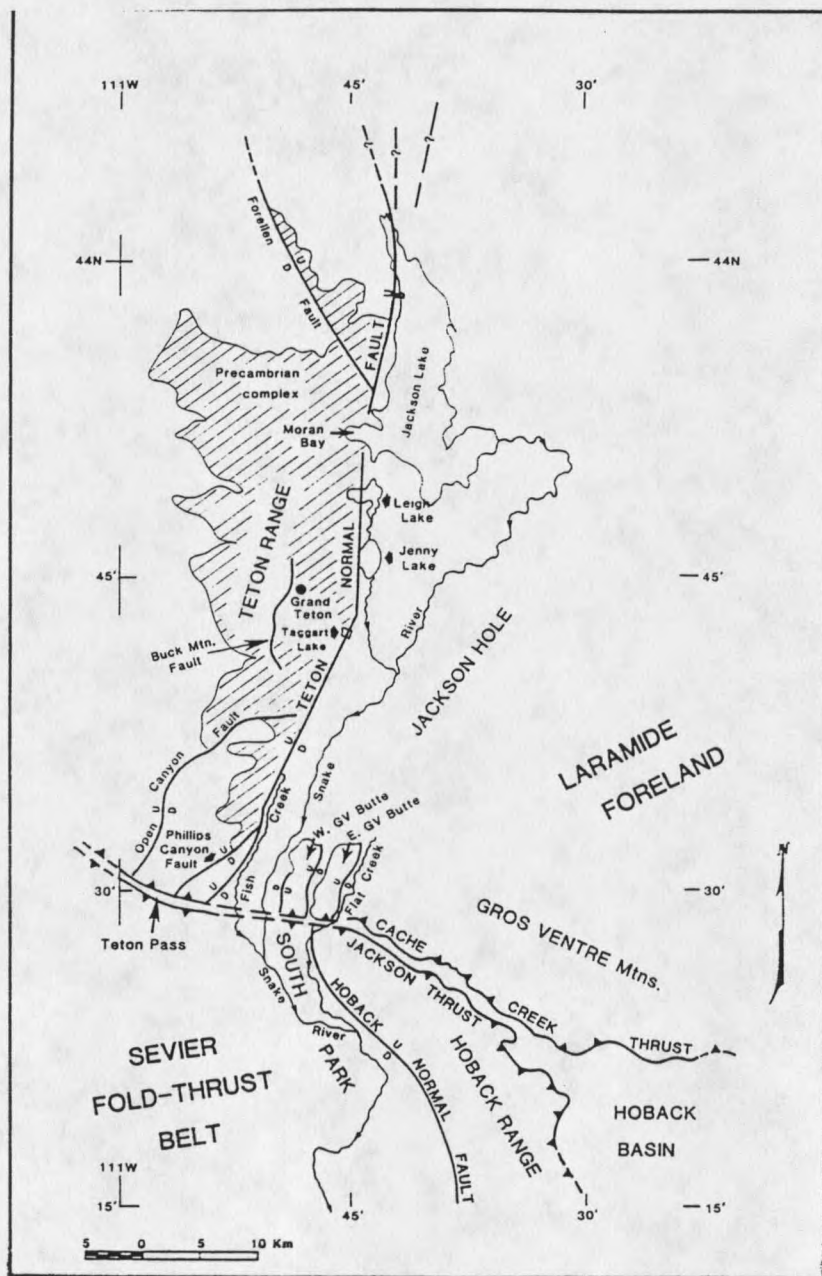


Figure 1. Structural index map of the Teton Range, reprinted from Lageson (1992).

imbricates of thin-skinned, Sevier-style thrusts, the Jackson-Prospect thrust being the northernmost. The episode of contractional tectonism that produced these structures lasted from late Cretaceous to perhaps early Eocene. The extensional tectonism which produced the Teton and Hoback faults and Jackson Hole itself commenced in the middle Miocene and continues to the present day (Byrd et al., 1994).

Considerable disagreement exists as to whether the Teton normal fault is confined to the Cache Creek thrust plate (i.e., soles into the Cache Creek decollement) or if it continues south of the province boundary (traced approximately by Wyoming Hwy. 22) into the region of the Sevier-style Snake River Range. It is of note that the Teton fault appears, as it approaches the edge of the Cache Creek thrust plate to the south, to shift from a single master fault, or fault zone, to a more distributed extensional system of normal faults. These faults, as mapped from west to east, are the Open Canyon fault, the Phillips Canyon fault, the Teton fault, and the faults bounding the east sides of the West and East Gros Ventre Buttes (Figure 1). Also present are several east-west faults, the Rendezvous Peak fault, the Warm Springs fault, and the Cache Creek fault, which may have served as transform structures accommodating differential extension in the area. It is this area of distributed extension that contains the bulk of the Jackson Hole volcanic complex.

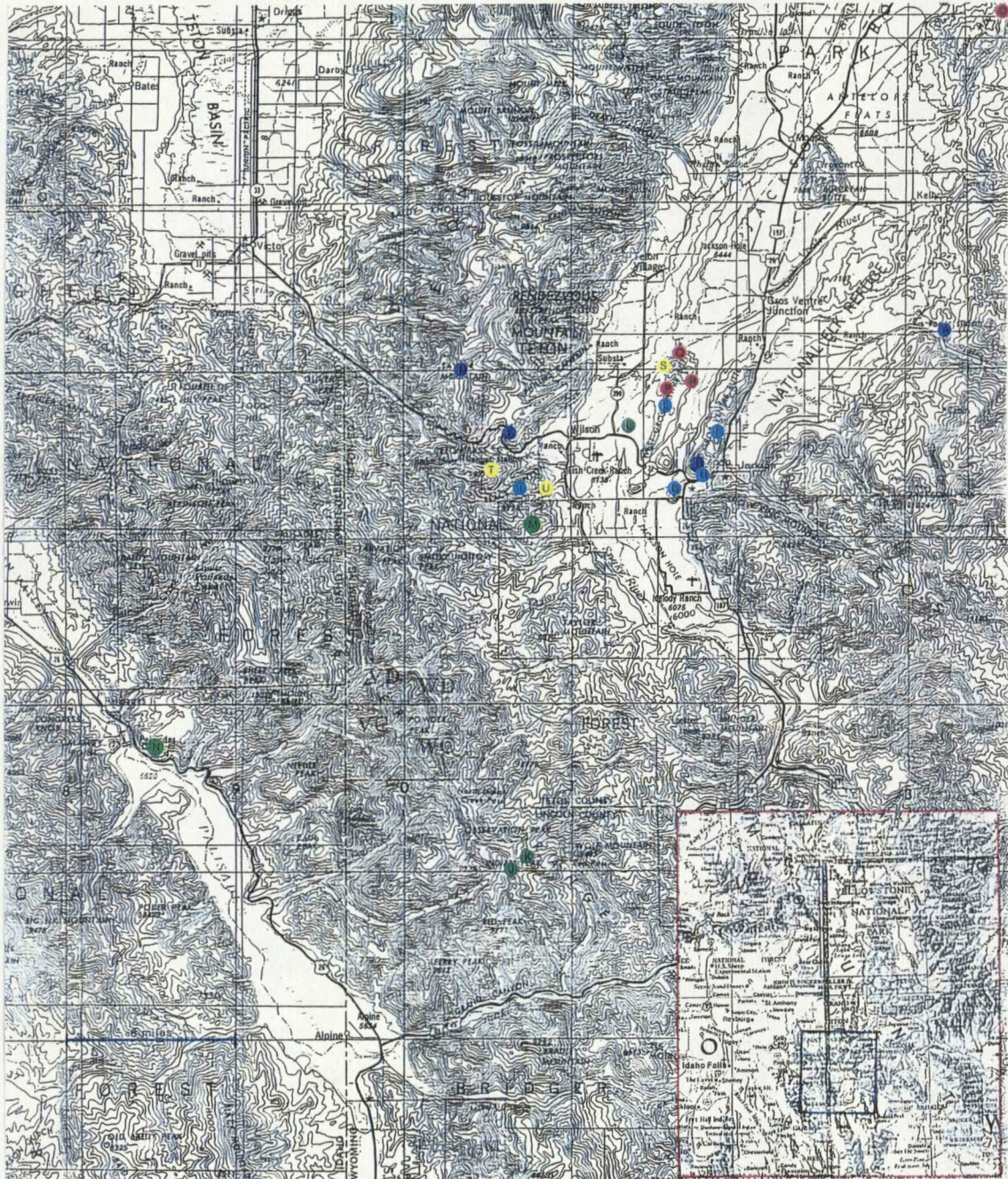


Figure 2. Map of study area, adapted from USGS Map NK 12-2, Western United States 1: 250000, Driggs, Idaho; Wyoming. Site labels correspond to samples listed in Tables 1-6.

Previous Work

Early work in southern Jackson Hole was done by Blackwelder (1915) and Fryxell (1930), with emphasis on the geomorphology of the area. Earlier studies on the structure of the Teton Range as a whole were performed by Horberg et al. (1949) and Edmund (1956). Geologic mapping in the vicinity of the study area was performed by Albee (1968; 1973), Schroeder (1969; 1972; 1974; 1976), Pampeyan et al. (1967), Love and Albee (1972), Love and Reed (1975), Oriel and Moore (1985), and Love et al. (1992). Interpretations of the geologic history of the area have been published by Love and Reed (1971) and Love et al. (1973). The Bureau of Reclamation has investigated local geology as part of seismotectonic studies in regard to construction on the Palisades Dam (Piety et al., 1986) and the Jackson Lake Dam (Gilbert et al., 1983). Other geophysical investigations in Jackson Hole have been carried out by Behrendt et al. (1968), Doser and Smith (1983), Smith et al. (1977), Smith et al. (1992), and Byrd et al. (1994). Structural studies have been conducted in the vicinity of Teton Pass by Zeller (1982), Vasko (1982), Lamerson (1983), and Dunn (1983); and further north in the Teton Range by Smith (1990), Smith et al. (1991), Lageson (1987; 1992), and Erslev and Rogers (1993). Geochronologic studies in the area have been performed by Evernden et al. (1964), Condie et al. (1969), Reed and Zartman (1973), Naeser et al. (1980), Armstrong et al. (1975) and Armstrong et al. (1980). Petrologic studies on the Precambrian rocks of the

area have been conducted by Horberg and Fryxell (1942), Bradley (1956), Miller et al. (1986), and Hildebrandt (1989).

Studies on Tertiary deposits in Jackson Hole have been done by Love (1956a, 1956b, 1956c, 1960, 1973, 1977), Love and Taylor (1962), Love and Montagne (1956), Lindsay (1972), Davis and Wilkinson (1983), Olsen and Schmitt (1987), Schmitt (1987), and Simons et al. (1988). Those with paleontological emphasis include Sohn (1956), Taylor (1956), C.W. Barnosky (1984), A.D. Barnosky (1985, 1986), Burbank and Barnosky (1990), and Whitlock (1992). Those with Quaternary emphasis include Glenn et al. (1983), Harrington (1985), Mahaney and Spence (1990), and Pierce and Good (1992). And those studies with significant mention of Cenozoic volcanic deposits include Scopel (1949, 1956), Houston (1956), Christiansen and Love (1978), Love et al. (1976), Love et al. (1978), Ritchie (1981), Love (1983), Barnosky (1984), Love (1986), and Perkins and Nash (1994).

Distribution of Volcanic Rocks

Volcanic deposits of various ages and various sources, both known and unknown, exist in the Jackson Hole area. Ash and breccias from Eocene Absaroka volcanic centers are abundant to the northeast of the valley and may extend southward in limited amounts. The Colter Formation, faunally dated as early to middle Miocene (Barnosky, 1984), lies primarily in the northern part of the valley but extends southward to the northern edge of the study area. Portions of this formation have been identified as pyroclastic surge

deposits; however, no evidence of an eruptive center, which should lie within 30 to 40 km, has been found.

The Teewinot Formation, faunally and K-Ar dated (Evernden et al., 1964) as middle Miocene (~10 Ma), lies to the immediate north of the study area. It consists of a substantial thickness of waterlain volcanic ash and freshwater limestone and marl. Recently, this ash has been correlated with that in the lacustrine middle Camp Davis Formation, which lies at the very southern end of the valley, and both have been re-dated (^{40}Ar - ^{39}Ar , ~7Ma). The source of these ashes is uncertain but may be twofold. Trace element studies (Ritchie, 1981; Love, 1986) suggest that one source type bears a resemblance to many other regional ash deposits and may be related to activity on the Snake River Plain. The other source type resembles the trace element trend of the JHV.

Other evidence of Yellowstone-Snake River Plain (YSP) volcanism is common throughout the valley. The Conant Creek Tuff (~4.5 Ma) is exposed in the northern part of the valley, as is the extremely voluminous Huckleberry Ridge Tuff (~2.0 Ma). Pinkish tuff resembling the latter is common near Teton Pass in the western part of and in the Signal and Shadow Mountain areas to the north and northeast of the study area.

Outcrops of the JHV are found primarily in the area of Teton Pass and the East and West Gros Ventre Buttes. Samples from Teton Pass have K-Ar whole-rock age determinations of $8.06 \pm .08$ Ma (rhyolite), $8.48 \pm .08$ Ma (obsidian) (Naeser et al., 1980), and 8.1 ± 0.9 Ma (basaltic andesite) (Chevron USA written comm., 1985, in Love,

et al., 1992). As is typical of more silicic lavas, these flows are not laterally extensive, and flows of differing lithology are seldom in stratigraphic contact. In addition, Miocene to recent extension has further separated the various outcrops on isolated fault blocks. In fact, the close geochemical correlation between the basaltic andesite capping the East Gros Ventre Butte above the town of Jackson with the aforementioned dated basaltic andesite on Teton Pass provides the first real maximum age for extensional tectonism in the southern Teton Range. The previous estimate was based on the absence of coarse-grained (i.e. orogenically derived) sediments in the middle Miocene Teewinot Formation (Love et al, 1973).

The absence of clear stratigraphic relationships between the various outcrops makes morphological reconstruction of the original volcanic field difficult. Without extensive and highly precise dating, even the sequence of eruptive events is uncertain. Extensive glaciation has not only eroded much of the original volcanic material but has perhaps also buried a substantial portion of the complex beneath the abundant glacial outwash that covers the valley floor and the lower slopes of the surrounding ranges. The original volcanic field may have existed as a group of isolated to slightly overlapping silicic domes and more laterally extensive andesitic flows erupted onto a surface of moderate relief and appears to have been structurally controlled more by the reactivated (?) east-west trending Laramide thrust faults than by the north-south Teton fault system.

The full spatial extent of the JHV is yet to be established. As chemical analyses are performed on various previously unsampled volcanic outcrops in the region, many show a

much stronger affinity to the JHV (or possibly to the Absaroka volcanics) than to the lavas of the YSP system. To the southwest of the main study area, at Palisades Dam, the Andesite of Calamity Point (K-Ar, whole rock, 6.3 ± 0.2 Ma, Armstrong et al., 1980) is essentially identical to a dacite flow south of Teton Pass. A block and ash flow exposed near Shadow Mountain northeast of the main study area is chemically very similar to the dacite flow covering the northern ends of the Gros Ventre Buttes, but could also be a remnant of Eocene volcanism. The hornblende-rich andesites found to the southwest of West Gros Ventre Butte and to the south of the study area at Indian Peak bear even more resemblance to the Eocene Absaroka group, but extensive crustal contamination, as evinced by abundant xenoliths, probably precludes successful dating or isotope analysis.

Given their general similarity, it is quite possible that more representatives of the Miocene calc-alkaline volcanic episode exist undated and undetected in the Absaroka calc-alkaline volcanics to the northeast. Lavas dated as Pliocene (K-Ar, 3.6 ± 1.0 Ma, Blackstone, 1966) in the Crescent Mountain area of the southern Absaroka Range show a much closer chemical affinity to the Jackson Hole Volcanics than Yellowstone lavas. And many other Neogene flows in this area (e.g. the Crandall Creek volcanics, Lava Mountain, and Pilot Knob) remain to be chemically analyzed and/or accurately dated. The actual extent and volume of Neogene calc-alkaline volcanism here may likely never be determined. It is, nonetheless, safe to say that the JHV and related lavas are in this regard dwarfed by both the Absaroka and Yellowstone-Snake River Plain systems. But relative volume should never be taken as a measure of significance.

CHAPTER 3

MATERIALS AND METHODS

Samples of the least altered material possible were always collected directly from the outcrop. Portions of 25 samples were sent to the GeoAnalytical Laboratory at Washington State University, where they were ground in a tungsten-carbide swingmill and analyzed on a 2:1 lithium tetraborate: rock powder fused bead using an automatic Rigaku 3370 spectrometer (Hooper et al., 1993). For 10 samples, portions of the same rock powder were sent to James Wright at Rice University, Houston, Texas, for analysis of isotope ratios for Sr, Rb, Sm, Nd, and Pb. Standards used and analytical uncertainties are listed in Table 2 of Wright and Snoke (1993).

Blocks were cut from these and other samples and sent to Spectrum Petrographics in Winston, Oregon, for preparation of 71 thin sections, of which 11 received microprobe polish treatment. These latter slides were analyzed at the Imaging and Chemical Analysis Laboratory at Montana State University, Bozeman, Montana, using a JEOL scanning electron microscope equipped for X-ray analysis. Chemical analyses were plotted graphically using Igpct For Windows (version 1-6-95) developed by Terra Softa Inc., Somerset, New Jersey.

CHAPTER 4

RESULTS

Overview

The rocks of the Jackson Hole Volcanic Complex can be subdivided into six basic groups based primarily on SiO_2 content. Names are based roughly on the classification scheme of LeBas et al. (1986) (Figure 3). These are as follows:

- 1) basaltic andesites - SiO_2 52-55%; olivine, augite, plagioclase, \pm enstatite;
- 2) low-silica andesites - SiO_2 56-59%; augite, plagioclase, \pm olivine, \pm enstatite-bronzite;
- 3) trachyandesites - SiO_2 53-61%; hornblende, plagioclase, augite; xenolith-rich (amphibolite and hornblendite);
- 4) high-silica andesites - SiO_2 62-64%; hypersthene, plagioclase, augite; or aphyric;
- 5) dacites - SiO_2 66-69%; plagioclase, hypersthene, \pm biotite, \pm augite;
- 6) rhyolites - SiO_2 73-75%; obsidian and aphyric (\pm plagioclase, \pm biotite).

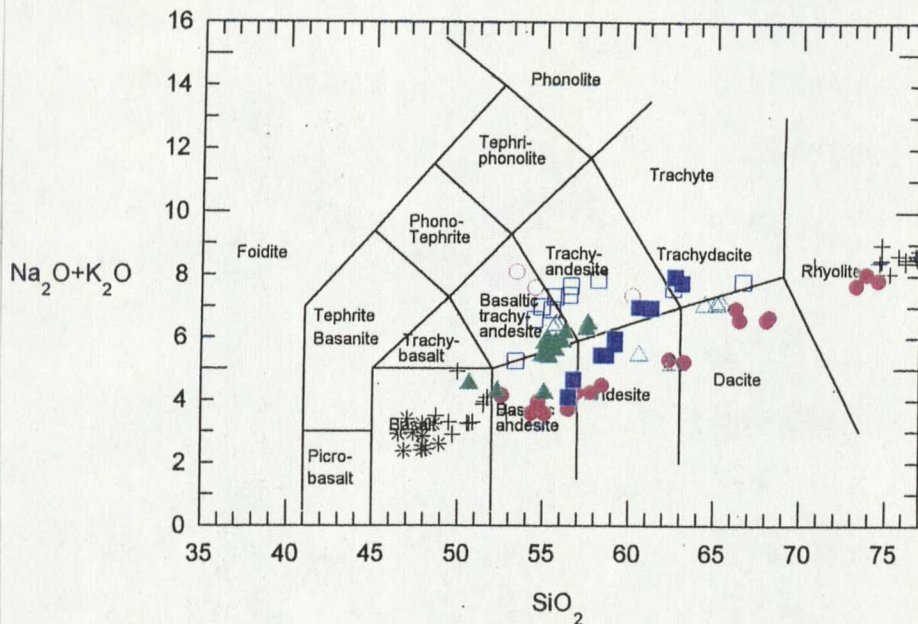


Figure 3. Total alkali vs. SiO_2 classification plot (LeBas et al., 1986) for the JHV and selected regional suites. Data from the Plio-Pleistocene Yellowstone Plateau Volcanic Field (YSP) (Hildreth et al., 1991) are plotted as black crosses (Yellowstone National Park) and asterisks (Island Park, Idaho). The Eocene Challis and Salmon Creek volcanics (SCV) (Norman and Mertzman, 1991) are plotted respectively as solid and hollow green triangles. The Cretaceous (most likely Eocene ?) Independence Peak volcanic rocks (Meens and Eggler, 1987) are plotted as solid (HABS-type) and empty (HATS-type) blue squares. The JHV are plotted as solid red circles with the intrusive andesites as hollow circles.

Locations and Field Characteristics

Basaltic Andesites

These flows are mainly found capping two fault blocks directly north of Teton Pass which are the hanging-wall blocks of the Open Canyon and Phillips Canyon faults, and the flows are clearly cut and displaced by at least the latter. Maximum thickness of

the flows is ~20 m., and they tend to be massive with only minimal flow foliation developed. They are directly underlain by limestones, shales, and cherts ranging from Mississippian to Permian in age. Samples were collected from the head of a Phillips Creek tributary near the pass between Mesquite and Coal Creeks (JH1) and from a large road cut on Hwy. 22 near Phillips Canyon (JH2). These lavas were not detected south of the highway (i.e. south of the Cache Creek thrust).

Basaltic andesite of almost identical chemical character is also found in an ~5 m thick outcrop capping the extreme southern end of the East Gros Ventre Butte, overlooking the town of Jackson (Sample JH5). This flow is highly foliated (~subvertical) and grades abruptly downward into low-silica andesite with an intervening zone apparently consisting either of mixing of two viscous magmas or of mixed and remelted flow-top rubble from the former and basal breccia from the latter. The much harder basaltic andesite domains tend to weather out as knobs. Also present to the immediate northeast of this outcrop are abundant fragments of black and red scoria.

The close chemical similarity between JH5 and the Teton Pass samples suggests that they are parts of essentially the same flow or, at least, flows not greatly separated temporally. However, flows at the mouth of Flat Creek Canyon (Sample 81) to the northeast of the East Gros Ventre Butte show sufficient differences that, although most likely part of the same magmatic episode, these lavas may represent the products of a separate magma chamber from the basaltic andesites to west. The Flat Creek lavas have also been extensively contaminated by secondary calcite, making comparison of major

Sample	81cc A	JH5 B	JH2 C	JH1 D
SiO[2]	52.58	54.33	54.74	55.12
Al[2]O[3]	14.88	16.12	15.85	16.76
TiO[2]	1.548	0.594	0.632	0.633
FeO*	10.4	6.79	6.7	6.73
MnO	0.125	0.119	0.114	0.122
CaO	10.58	9.1	8.99	8.62
MgO	5.31	8.73	8.38	7.95
K[2]O	1.07	0.83	1	0.73
Na[2]O	3.07	2.75	2.93	2.84
P[2]O[5]	0.408	0.218	0.432	0.181
Mg*	47.6	69.6	69	67.8
Ni	161	204	208	180
Cr	286	551	522	540
Sc	27	18	22	28
V	171	137	126	132
Ba	881	662	1223	555
Rb	14	11	12	12
Sr	915	510	954	465
Zr	160	121	138	108
Y	20	18	21	18
Nb	12.6	7.1	7.6	8.9
Ga	22	19	14	18
Cu	53	32	37	36
Zn	99	71	69	75
Pb	5	6	12	5
La	54	41	69	25
Ce	124	67	115	55
Th	7	2	5	4
87Sr/86Sr		.706102(7)	.706460(9)	.706491(8)
143Nd/144		.511575(5)	.511483(5)	.511675(5)
208Pb/204		37.769	37.309	38.322
207Pb/204		15.476	15.377	15.466
206Pb/204		16.913	16.494	17.069

Major element values for 81cc adjusted for calcite contamination
Mg* = 100 Mg/(Mg + Fe) atomic

Table 1. Major and trace element contents and isotope ratios for basaltic andesite samples.

elements somewhat difficult and isotope analysis impossible, but leaving some trace elements arguably unaffected.

Low-silica Andesites

As mentioned previously, these lavas are found underlying basaltic andesites at the extreme southern end of East Gros Ventre Butte, where the flow attains a thickness of 25-30 m. Portions of this flow (Sample JH3) have subsequently been downdropped to the level of Broadway/ Highway 189 by the west-trending normal fault that bounds the south end of the butte. Parts of perhaps the same flow are found in a small outcrop to the southwest on Haystack Butte (Sample JH9) which is part of the Jackson thrust sheet.

Low-silica andesites are also found in the central portions of both East (Sample JH11) and West GrosVentre Buttes (Sample 617). These rocks have well-developed flow foliation in almost all exposures and occasional columnar jointing. A small outcrop approximately 4 km. southeast of Teton Pass (Sample 519) falls within this range of silica content and shares similar petrographic characteristics, but its trace element contents suggest it may not be closely related to the other low-silica andesites.

Sample	JH617 E	JH11 F	JH9 G	JH3 H	JH519 I
SiO ₂	56.48	56.66	56.96	57.81	58.44
Al ₂ O ₃	16.99	17.34	17.33	17.55	16.81
TiO ₂	0.635	0.638	0.633	0.611	0.951
FeO*	6.85	6.44	6.13	5.95	6.67
MnO	0.108	0.108	0.098	0.102	0.116
CaO	8.35	8.26	8.09	8.15	7.1
MgO	6.37	5.74	5.51	5.35	4.33
K ₂ O	0.92	1.03	0.99	1.01	1.05
Na ₂ O	2.8	3.02	3.24	3.23	3.42
P ₂ O ₅	0.132	0.17	0.213	0.202	0.404
Mg*	62.4	61.3	61.5	61.5	53.6
Ni	135	113	107	89	77
Cr	315	226	243	178	131
Sc	25	19	19	18	23
V	138	130	104	118	122
Ba	492	574	1101	699	1066
Rb	17	18	16	16	12
Sr	286	346	474	437	547
Zr	106	111	138	136	189
Y	20	21	23	20	31
Nb	4.9	8.2	9.9	9.2	16.2
Ga	19	17	16	18	16
Cu	47	45	37	30	14
Zn	69	72	70	66	94
Pb	5	8	11	9	3
La	17	13	32	30	48
Ce	59	64	76	68	69
Th	2	2	6	2	6
⁸⁷ Sr/ ⁸⁶ Sr		.706668(8)		.706245(9)	
¹⁴³ Nd/ ¹⁴⁴		.511690(4)		.511579(5)	
²⁰⁸ Pb/ ²⁰⁴		37.863		37.446	
²⁰⁷ Pb/ ²⁰⁴		15.409		15.409	
²⁰⁶ Pb/ ²⁰⁴		16.47		16.638	

Mg* = 100 Mg/(Mg + Fe) atomic

Table 2. Major and trace element contents and isotope ratios for low-silica andesite samples.

Trachyandesites

These lavas are present in a small outcrop west of the West Gros Ventre Butte near the Hwy. 22 bridge over the Snake River (Sample JH17) and in a much larger hypabyssal intrusive complex at Indian Peak approximately 25 km to the south-southeast in the Snake River Range (Samples IPK2 and IPK6). Although there is a fairly wide range in silica content between the samples, their petrographic similarity and presence of abundant hornblende and lower-crustal xenoliths suggests that they are of similar origin. Xenoliths, however, preclude both dependable dating and isotope analysis. Based on their greater petrographic and geochemical similarity to the Absaroka volcanic rocks, these rocks are probably Eocene rather than Miocene in age.

High-silica Andesites

This silica range is represented by two flows that are chemically almost identical. One (Sample JH10) is located ~6 km southeast of Teton Pass capping the ridge directly north of Mosquito Creek. The other (Sample 640) lies ~25 km to the southwest, slightly to the southeast of the east abutment of the Palisades Dam. This latter flow, dated by Armstrong et al. (1980) at 6.3 ± 0.2 Ma, is ~60 m thick and tends to be slightly more massive than the thinner (~20 m?) Mosquito Creek flow which shows well-developed platy weathering due to flow foliation. Although separated by considerable distance and

Sample	IPK6 J	IPK2 K	JH17 L
SiO[2]	53.4	54.5	60.18
Al[2]O[3]	19.47	19.14	17.23
TiO[2]	0.495	0.506	0.559
FeO*	5.84	6.18	5.9
MnO	0.089	0.129	0.08
CaO	8.19	8.82	5.1
MgO	1.82	2.42	2.52
K[2]O	3.88	3.62	2.78
Na[2]O	4.22	3.98	4.57
P[2]O[5]	0.336	0.302	0.362
Mg*	35.7	41.1	43.2
Ni	7	13	26
Cr	15	43	62
Sc	17	16	15
V	89	98	121
Ba	452	414	924
Rb	92	92	58
Sr	1114	1003	876
Zr	195	183	171
Y	28	28	26
Nb	10	8.2	11.9
Ga	20	20	18
Cu	23	35	38
Zn	52	75	83
Pb	3	22	14
La	40	32	33
Ce	93	92	40
Th	12	9	3

Mg* = 100 Mg/(Mg + Fe) atomic

Table 3. Major and trace element contents and isotope ratios for trachyandesite samples.

Sample	JH10 M	JH640 N
SiO ₂	62.37	63.27
Al ₂ O ₃	16.89	16.85
TiO ₂	0.669	0.649
FeO*	5.15	5.39
MnO	0.086	0.083
CaO	5.95	5.75
MgO	2.61	2.7
K ₂ O	1.66	1.48
Na ₂ O	3.64	3.73
P ₂ O ₅	0.194	0.181
Mg*	47.5	47.1
Ni	32	21
Cr	73	56
Sc	18	16
V	94	98
Ba	737	768
Rb	32	24
Sr	284	289
Zr	170	176
Y	28	28
Nb	10.8	10.7
Ga	18	23
Cu	18	15
Zn	71	68
Pb	11	9
La	38	101
Ce	65	61
Th	7	4
⁸⁷ Sr/ ⁸⁶ Sr	.707731(8)	
¹⁴³ Nd/ ¹⁴⁴ Nd	.511591(9)	
²⁰⁸ Pb/ ²⁰⁴ Pb	38.41	
²⁰⁷ Pb/ ²⁰⁴ Pb	15.463	
²⁰⁶ Pb/ ²⁰⁴ Pb	16.653	

Mg* = 100 Mg/(Mg + Fe) atomic

Table 4. Major and trace element contents and isotope ratios for high-silica andesite samples.

different petrographically (unlike 640, JH10 is aphyric), the close chemical similarity suggests these flows may be co-magmatic, if not parts of the same flow.

Dacites

These lavas are present as thick flows (> 300 m) which essentially comprise the northern ends of both the East and West Gros Ventre Buttes, and are of two fundamental types. The dominant lithology is a porphyritic dacite with andesine phenocrysts up to 3 mm in length in a dark gray to black (often red) matrix. These flows are massive to moderately foliated with rare columnar joints. They are quarried for dike rip-rap at the extreme north end of the West Gros Ventre Butte (Sample JH7). They form the top of Hansen Peak (the highest point of the West Gros Ventre Butte) and the prominent cliffs on the east side of the East Gros Ventre Butte.

The slightly less silicic and less voluminous non-porphyritic dacites (Sample JH12) crop out to the south of Hansen Peak and appear to underlie the porphyritic dacites with an non-planar northward-dipping contact. They are distinctly more foliated than the porphyritic dacites and become slightly more porphyritic towards the east, where an apparent vent structure forms a large plug-like outcrop comprised of non-porphyritic dacite blocks up to several meters across (vent breccia ?) suspended in densely porphyritic dacitic matrix (Sample JH6). Just north of this plug are scattered perlite clasts, possibly

Sample	SM4 O	JH12 P	JH7 Q	JH6 R
SiO ₂	66.28	66.49	68.06	68.21
Al ₂ O ₃	15.96	16.36	15.67	15.82
TiO ₂	0.44	0.595	0.504	0.463
FeO*	3.49	3.67	3.6	3.35
MnO	0.019	0.048	0.066	0.064
CaO	4.11	4.3	3.7	3.85
MgO	1.68	0.68	0.86	0.94
K ₂ O	2.83	2.42	2.42	2.61
Na ₂ O	4.11	4.15	4.15	4.05
P ₂ O ₅	0.179	0.191	0.152	0.139
Mg*	46.2	24.9	29.8	33.3
Ni	54	7	6	7
Cr	126	1	7	5
Sc	13	7	9	6
V	66	56	50	63
Ba	1649	844	864	866
Rb	60	62	57	64
Sr	636	270	239	244
Zr	148	160	172	151
Y	11	30	27	27
Nb	5.3	11.1	12.2	14.2
Ga	20	21	19	18
Cu	15	10	5	9
Zn	54	60	59	53
Pb	21	20	15	21
La	14	44	39	46
Ce	71	79	83	74
Th	4	10	13	10
⁸⁷ Sr/ ⁸⁶ Sr		.710403(8)	.709265(8)	
¹⁴³ Nd/ ¹⁴⁴ Nd		.511508(5)	.511547(4)	
²⁰⁸ Pb/ ²⁰⁴ Pb		40.019	39.093	
²⁰⁷ Pb/ ²⁰⁴ Pb		15.527	15.583	
²⁰⁶ Pb/ ²⁰⁴ Pb		16.908	17.352	

Mg* = 100 Mg/(Mg + Fe) atomic

Table 5. Major and trace element contents and isotope ratios for dacite samples.

remnants of the glassy chilled intrusive margin. Non-porphyrific dacite has not been found on the East Gros Ventre Butte.

Scopel (1949, 1956) reported lavas as having flowed down the steep eastern sides of the buttes, thus making magmatism post-kinematic. It is clear, however, that these dacitic flows were extremely thick (i.e. dome-like) which is common for phenocryst-rich silicic lavas. Flow foliations are predominantly west-dipping, clearly contrary to flow down these east-dipping fault surfaces. The dacite exposed in these surfaces is therefore most likely pre-kinematic in origin, and the dacites of the two buttes probably formed one large composite dome.

Approximately 25 km to the northeast of the Gros Ventre Buttes, on Ditch Creek east of Shadow Mountain, a monolithologic, block and ash flow deposit (Sample SM4) is very similar in chemistry and phenocryst content to the dacites to the south. However, certain key major and trace elements are sufficiently different as to preclude any direct connection between this flow and those of the buttes. This flow is, nonetheless, much more closely related to the JHV than to the Absaroka volcanic rocks, let alone those of Yellowstone.

Rhyolites

Rhyolitic flows are present south of Teton Pass, on West Gros Ventre Butte, and, to a very limited extent, on East Gros Ventre Butte. Obsidian is found in areally limited

Sample	JH15 S	JH14 T	JH13 U
SiO[2]	73.26	73.83	74.53
Al[2]O[3]	15.28	14.07	14.46
TiO[2]	0.241	0.07	0.068
FeO*	1.75	1.02	0.94
MnO	0.04	0.049	0.016
CaO	2.13	1.38	1.24
MgO	0.1	0	0
K[2]O	3.46	3.95	4.11
Na[2]O	4.22	4.1	3.74
P[2]O[5]	0.082	0.038	0.038
Mg*	9.3		
Ni	7	12	11
Cr	0	5	1
Sc	2	3	1
V	5	0	0
Ba	1156	1177	1214
Rb	88	121	124
Sr	185	125	114
Zr	188	73	70
Y	28	26	22
Nb	15.1	14.2	16.4
Ga	18	15	17
Cu	32	6	4
Zn	65	37	38
Pb	25	27	30
La	40	11	32
Ce	74	57	56
Th	13	14	14
$^{87}\text{Sr}/^{86}\text{Sr}$.711725(8)	.723476(8)	
$^{143}\text{Nd}/^{144}$.511528(4)	.511414(5)	
$^{208}\text{Pb}/^{204}$	40.116	41.548	
$^{207}\text{Pb}/^{204}$	15.542	15.622	
$^{206}\text{Pb}/^{204}$	16.948	17.364	

Mg* = 100 Mg/(Mg + Fe) atomic

Table 6. Major and trace element contents and isotope ratios for rhyolite samples.

“pipes” on ridges 1 km and 2 km (Sample JH14) southeast of Teton Pass, which have been the sites of prehistoric quarrying. It is also found in excavations and as a consistent subsurface layer in building site assessment drill cores and water wells up to 6 km southeast of the Pass. Tan-colored flow-banded rhyolite (Sample JH13) also crops out ~5 km southeast of the Pass at the base of Indian Paintbrush Subdivision. Samples from the same sites as JH13 and JH14 were dated at $8.06 \pm .08$ Ma and $8.48 \pm .08$ Ma, respectively (Naeser et al., 1980), and the nearly identical chemical composition of these two samples suggests that the rhyolite and obsidian may only be different textural variations of the same flow.

A dark gray and red flow-banded rhyolite (Sample JH15) is well exposed in a quarry on the west side of West Gros Ventre Butte. It is associated with a red and black breccia that is largely altered (hydrothermally ?) to a deep-reddish soil with occasional dark gray dacite (?) clasts and rare obsidian fragments. Foliation in the overlying non-porphyrific dacite is roughly sub-parallel to the contact with the underlying rhyolite body, suggesting that the rhyolite is either an intrusive plug deforming the intruded dacite or a pre-existing dome over which the dacite flowed. No sign is present of a chilled contact, which would confirm the former, but such a margin would be highly susceptible to alteration, of which there is ample evidence. JH15 is chemically similar to, yet distinct from, the flow(s) near Teton Pass and most likely represents a co-genetic but separate eruptive event.

On the east side of East Gros Ventre Butte, porphyritic dacite in places overlies thin beds of orange pumice and pumiceous sandstone. Petrographically, these units show signs of both epiclastic reworking (e.g. rounding) and welding (flattened pumice). As such, this pumice need not be related to the JHV. On Teton Pass, a reddish tuff (Sample JH18) appears to underlie the JH2 basaltic andesite and shows strong chemical affinity to the Yellowstone-Snake River Plain lavas. If it actually overlies the Miocene basaltic andesite, it could be Huckleberry Ridge Tuff, which it roughly resembles. In any case, it appears distinctly unrelated to the JVH.

Petrography

Basaltic Andesites

The basaltic andesites are phenocryst-rich (20 -30%). The dominant mineral phase is euhedral to subhedral olivine phenocrysts (Fo_{80-88} , molar %) up to 2.5 mm in length. They are commonly iddingsitized on their rims and along fractures (Figure 4), suggesting that this is a late-stage, low-temperature reaction (McMillan, pers. comm. 1996) but probably deuteric rather than a weathering product. Other samples (e.g. Sample 81) show signs of extensive replacement of olivine with fine-grained opaques, also along fractures (Figure 5).

Euhedral to subhedral augite phenocrysts up to 1.5 mm in length are slightly less abundant than the olivine. They range from $\text{Wo}_{38} \text{En}_{52} \text{Fs}_{10}$ (Sample JH2) to $\text{Wo}_{44} \text{En}_{43} \text{Fs}_{13}$ (Sample 81) and are often in glomerocrysts associated with plagioclase. Sample JH5

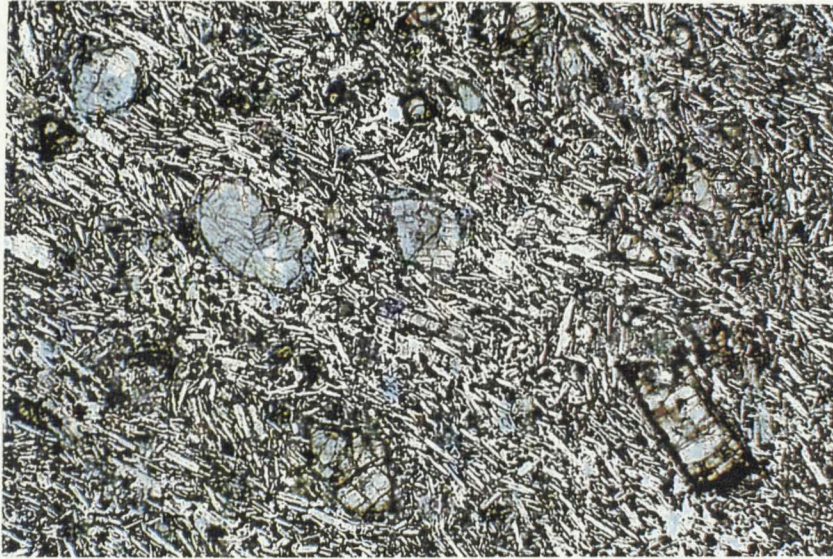


Figure 4. Photomicrograph of Sample JH1 (plane polarized light (PPL), 17x). Olivines show alteration to reddish brown iddingsite; whereas the pale green augite phenocrysts do not.



Figure 5. Photomicrograph of Sample 81 (PPL, 85x). Olivine phenocryst altered to fine-grained opaques.

contains rare bronzite phenocrysts ($Wo_2 En_{81} Fs_{17}$). These are up to 1.0 mm in length and show irregular exsolution lamellae of augite(?).

Bytownite laths (An_{74}) up to 1.5 mm in length are common, although most plagioclase crystals are present as groundmass laths and microlites with a pilotaxitic to trachytic texture. The plagioclase also appears reasonably fresh and is normally zoned. Aside from the microlites, the matrix contains fine-grained pyroxene, scattered opaques, and some glass. As previously mentioned, Sample 81 from Flat Creek shows signs of extensive vesicle infilling with secondary calcite and silica.

Low-silica Andesites

These rocks are generally less phenocryst-rich than the basaltic andesites, usually with <20 vol.% and as little as 4 vol.% in Sample JH11. Olivine in these samples is corroded and rimmed with, or entirely replaced by, orthopyroxene (Figure 6). Bronzite phenocrysts ($Wo_3 En_{74} Fs_{23}$) up to 2.0 mm in length are common. Augite phenocrysts ($Wo_{42} En_{43} Fs_{15}$) are slightly smaller and less abundant. Both pyroxenes are abundant in the groundmass.

Plagioclase (An_{74}) is uncommon as large phenocrysts; it is mainly present as small laths and microlites that comprise the bulk of the moderately to strongly trachytic groundmass. Occasional larger plagioclase phenocrysts up to 2 mm are often corroded with sieve-textured cores. Glass in the matrix ranges from none (Samples JH3 and JH11) to moderate (Samples 617 and 519).

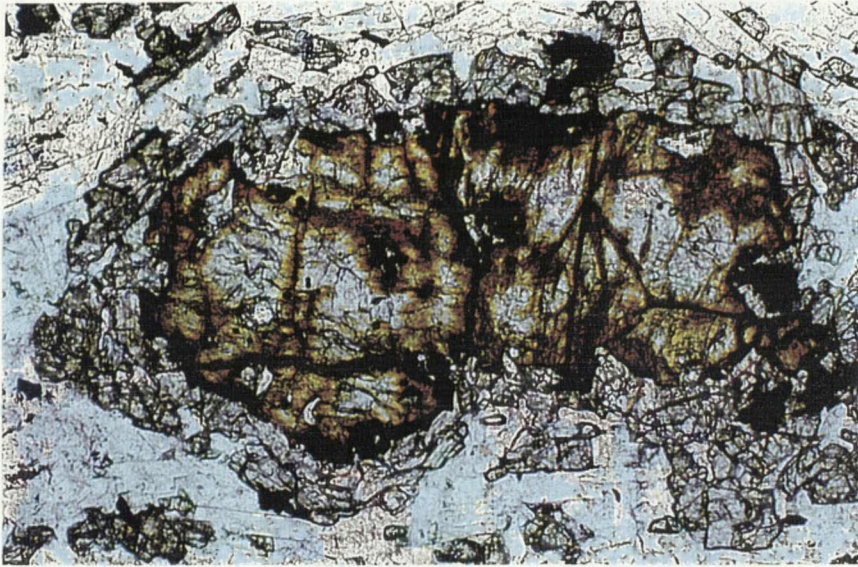


Figure 6. Photomicrograph of Sample 625 (PPL, 85x). Corroded and iddingsitized olivine rimmed with orthopyroxene.

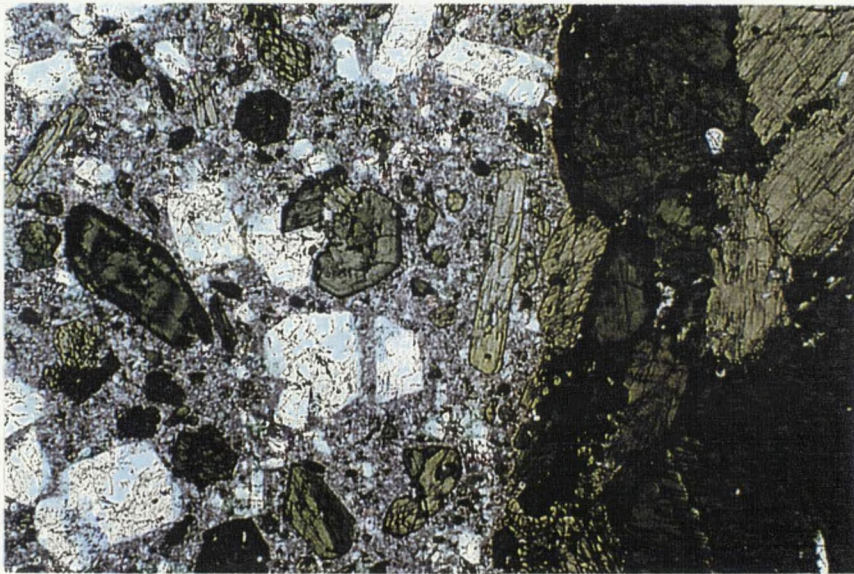


Figure 7. Photomicrograph of Sample 606 (PPL, 17x). Hornblende with oscillatory zoning and rounded plagioclase at left. Hornblendite xenolith at right.

Trachyandesites

These rocks are generally richer in phenocrysts (up to 55%) than the other groups, but their most distinctive petrographic feature is the presence of hornblende, which is absent from other JHV rocks but common in Absaroka volcanic rocks. It is perthitic in nature and indistinguishable from amphibole crystals in the numerous hornblendite xenoliths present in all the samples (Figure 7). These xenoliths also contain limited amounts of pyroxene and rare garnet, suggesting a lower crustal origin (Green, 1982). Although some of the hornblende crystals may be xenocrysts derived from disaggregated xenoliths, many show overall normal (i.e. Fe/Mg increases from core to rim) oscillatory zoning, which suggests a magmatic rather than metamorphic origin. Further evidence of the complex history of this extensively contaminated magma is seen, on the one hand, in hornblende(?)-rimmed clinopyroxenes (especially within the xenoliths) versus the disequilibrium association of corroded hornblende with fresh, euhedral clinopyroxene (away from the xenoliths) on the other hand.

Plagioclase also shows numerous disequilibrium features (i.e. resorption, fritting, calcic overgrowths, etc.). As in the hornblende crystals, many of these may be due to magma mixing (Stimac and Pearce, 1992) or, more likely, to rapid decompression. Rapid ascent from the lower crust, as postulated by Green (1982), could produce both pressure instability of hornblende and sieve-cored and fritted textures in plagioclase (Nelson and Montana, 1992).

High-silica Andesites

These samples, although chemically quite similar, show marked petrographic differences. The Mosquito Creek flow (Sample JH10) is aphyric with only small plagioclase microlites in a mottled matrix probably due to partial devitrification of the original glass. The Palisades Dam andesite has a similar groundmass but also contains numerous glomerocrysts consisting of plagioclase and clinopyroxene.

Dacites

The large (up to 5 mm in length) andesine phenocrysts, which distinguish the porphyritic from the non-porphyritic dacites on the Gros Ventre Buttes, show many of the same disequilibrium textures present in the trachyandesites. Overall, they are normally zoned (An_{48} core to An_{12} rim) but also show strong oscillatory zoning. They are noticeably rounded due to resorption, have sieve-textured cores (Figure 8), and show strong fritting with and without calcic(?) overgrowths (Figure 9). Plagioclase forms the bulk of the phenocryst content which ranges from 12-18 vol.% in the non-porphyritic and from 28-42 vol.% in the porphyritic dacites.

Subordinate to plagioclase are hypersthene ($Wo_2 En_{58} Fs_{40}$) phenocrysts up to 1.8 mm. in length. In addition, rare augite ($Wo_{45} En_{37} Fs_{18}$) is present but may be xenocrystic. The groundmass ranges from nearly holocrystalline comprised of mainly small plagioclase laths (Sample JH6) to nearly holohyaline comprised of dark brown glass (Samples JH7 and 32). The latter also shows acicular Fe-oxide pseudomorphs (after biotite?) and occasional rhomb-shaped pseudomorphs (after hornblende?)(Figure 10).

